

# Analysis of current distribution and termination conditions in 2D metasurfaces

Analysis of  
current  
distribution

Sami Barmada and Nunzia Fontana

*Department of Energy, Systems, Territory and Construction Engineering,  
Università di Pisa, Pisa, Italy, and*

Leonardo Sandrolini and Mattia Simonazzi

*Department of Electrical, Electronic, and Information Engineering “Guglielmo  
Marconi”, Alma Mater Studiorum Università di Bologna, Bologna, Italy*

Received 31 October 2023  
Revised 28 December 2023  
Accepted 29 January 2024

## Abstract

**Purpose** – The purpose of this paper is to gain a better understanding on how metasurfaces behave, in terms of currents in each unit cell. A better knowledge of their behavior could lead to an ad-hoc design for specific applications.

**Design/methodology/approach** – The methodology used is both theoretical and numerical; it is based on circuit theory and on an optimization procedure.

**Findings** – The results show that when the knowledge of the current in each unit cell of a metasurface is needed, the most common approximations currently used are often not accurate. Furthermore, a procedure for the termination of a metasurface, with application-driven goals, is given.

**Originality/value** – This paper investigates the distribution of the currents in a 2D metamaterial realized with magnetically coupled resonant coils. Different models for the analysis of these structures are illustrated, and the effects of the approximations they introduce on the current values are shown and discussed. Furthermore, proper terminations of the resonators on the boundaries have been investigated by implementing a numerical optimization procedure with the purpose of achieving a uniform distribution of the resonator currents. The results show that the behavior of a metasurface (in terms of currents in each single resonator) depends on different properties; as a consequence, their design is not a trivial task and is dependent on the specific applications they are designed for. A design strategy, with lumped impedance termination, is here proposed.

**Keywords** Particle swarm optimization, Metamaterials, Equivalent circuit model

**Paper type** Research paper

© Sami Barmada, Nunzia Fontana, Leonardo Sandrolini and Mattia Simonazzi. Published by Emerald Publishing Limited. This article is published under the Creative Commons Attribution (CC BY 4.0) licence. Anyone may reproduce, distribute, translate and create derivative works of this article (for both commercial and non-commercial purposes), subject to full attribution to the original publication and authors. The full terms of this licence may be seen at <http://creativecommons.org/licenses/by/4.0/legalcode>

This study was carried out within the MOST – Sustainable Mobility Center and received funding from the European Union Next-Generation EU (PIANO NAZIONALE DI RIPRESA E RESILIENZA (PNRR) – MISSIONE 4 COMPONENTE 2, INVESTIMENTO 1.4 – D.D. 1033 17/06/2022, CN00000023). This manuscript reflects only the authors' views and opinions, neither the European Union nor the European Commission can be considered responsible for them.



COMPEL - The international  
journal for computation and  
mathematics in electrical and  
electronic engineering  
Emerald Publishing Limited  
0332-1649

DOI 10.1108/COMPEL-10-2023-0548

## 1. Introduction

Metamaterials are a class of artificial materials characterized by peculiar electromagnetic properties. They are realized with magnetically coupled resonant coils – often called “unit cells” or “meta-atoms,” arranged in 2D or 3D arrays to form regular lattices. Metamaterials are widely exploited in the fields of microwaves and optics (Glybovski *et al.*, 2016) and have been recently considered in wireless power transfer (WPT) systems operating in near-field regions, where 2D arrays of resonators – sometimes referred as “metasurfaces” – are used to transmit or receive power, as well as to improve the transmission efficiency of the overall system (Sandoval *et al.*, 2019; Brizi *et al.*, 2020).

While the analysis of large-lattice metamaterials can be described by resorting to the theory of magneto-inductive waves (Solymar and Shamonina, 2009), in case of a limited number of unit cells, this theory may lead to inaccurate results, as shown in this contribution. A possibility to accurately analyze the metamaterial is to perform a circuit analysis that allows for evaluating the magnitudes of currents and voltages in each unit cell.

The usefulness of a uniform current distribution in the metasurface has been shown in different application fields; still referring to WPT systems (hence to specific dimensions and frequency of operation), in Lazzoni *et al.* (2023) it is demonstrated that the unit-cell current uniformity leads to a significantly more homogenous magnetic field distribution, fundamental to improve the WPT performance in terms of robustness to misalignment.

This paper investigates different approximations in the modelling of the metamaterial, still preserving a great accuracy. Furthermore, the effect of different characteristic parameters, such as quality factor of each unit cell, number of the unit cells, termination impedances, is investigated.

In addition to the study mentioned before, a procedure to determine the proper terminations of the resonators on the boundaries is investigated, with the purpose of levelling the magnitude of the resonators currents. This specific working conditions can be exploited in practical systems such as multireceiver WPT systems, where each unit cell is a receiver, or it is part of a 2D array where a pick-up receiving coil can be placed on any of the unit cells of the surface.

## 2. 2D metamaterial surface

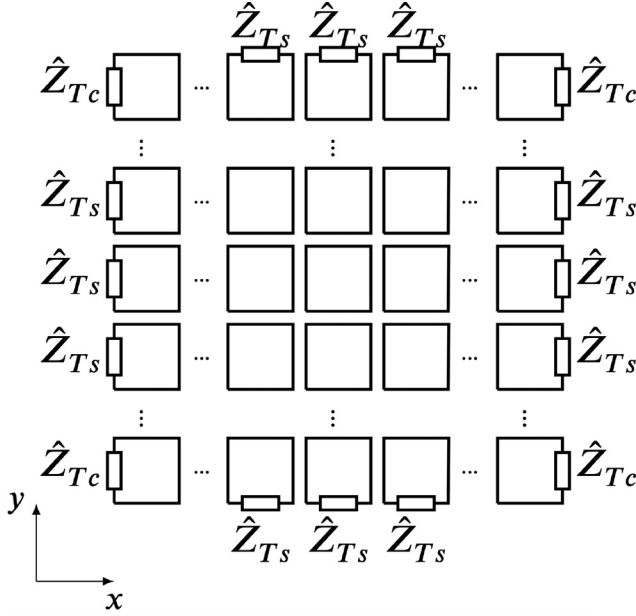
The considered metasurface is composed of  $N \times N$  resonant RLC coils immersed in a linear medium and arranged to form a square lattice, as represented in Figure 1, where  $\hat{Z}_{Ts}$  and  $\hat{Z}_{Tc}$  are lumped termination impedances in the edges and in the corners, respectively. In Barmada *et al.* (2022), three termination impedances were used, because of the focus was to work on a  $5 \times 5$  surface; in this contribution, the theoretical study is relative to a general metasurface, and the choice of only two termination impedances is the most logical one, being less prone to case dependency.

In many applications, the frequency range of operation of the metasurface makes it possible to express the relation between the currents circulating in the loops by the use of the well-known Kirchhoff Voltage Law (KVL). As it is common in applications characterized by the presence of metasurfaces, their performance is commonly in the frequency domain. For this reason, in this work, only sinusoidal steady-state regime is considered, and all the voltages and currents are represented by the respective phasors.

The resulting system of equations can be expressed in matrix form as:

$$\hat{V} = \hat{Z}_M \hat{I} \quad (1)$$

where  $\hat{Z}_M$  is the impedance matrix of the system,  $\hat{I}$  is the vector of the phasor currents flowing in the resonators and  $\hat{V} = [0, 0, \dots, \hat{V}_s, \dots, 0, 0]$  is the phasor voltage vector with  $\hat{V}_s$  being the voltage supply phasor; throughout the paper the analysis is carried out supposing excitation in the central resonator. Rigorously, the impedance matrix should



Analysis of  
current  
distribution

**Figure 1.**  
Schematic  
representation of the  
metasurface

**Source:** Figure created by authors

include the coupling coefficients between all the coils composing the metamaterial (Brizi *et al.*, 2020; Solymar and Shamonina, 2009) and is defined as:

$$\hat{\mathbf{Z}}_M = \begin{bmatrix} \hat{Z}_1 & j\omega M_{12} & j\omega M_{13} & \cdots & j\omega M_{1N} \\ j\omega M_{21} & \hat{Z}_2 & j\omega M_{23} & \cdots & j\omega M_{2N} \\ \vdots & \vdots & \vdots & \vdots & \vdots \\ \vdots & \vdots & \vdots & \vdots & \vdots \\ j\omega M_{N1} & \cdots & \cdots & j\omega M_{N(N-1)} & \hat{Z}_N \end{bmatrix} \quad (2)$$

The cell of the lattice in the generic position  $(m, n)$  is characterized by its self-impedance:

$$\hat{Z}_{m,n} = R_{m,n} + j \left( \omega L_{m,n} - \frac{1}{\omega C_{m,n}} \right) \quad (3)$$

where  $R_{m,n}$  is the resistance,  $L_{m,n}$  is the self-inductance and  $C_{m,n}$  is the capacitance of the coil. The value of  $C_{m,n}$  can be obtained either by connecting lumped capacitors to the magnetic coils or exploiting the coils self-capacitance with a proper design (Baena *et al.*, 2005). In particular, for low-frequency applications (up to a few GHz), the self-capacitances of the unit cells are too small and lumped capacitors are required to make the coils resonate at the desired frequency.

Considering all the elements wound in the same direction and coincident current references for all elements, in planar structures, the magnetic interaction of coplanar-coupled coils is characterized by a negative mutual inductance.

In the majority of applications, metasurfaces are designed to form periodic lattices; consequently, all coils are identical to each other and positioned such that their mutual inductance coefficients lead to a symmetric impedance matrix  $\hat{\mathbf{Z}}_M$ .

The resonators composing the metasurfaces considered in this paper are characterized by a resistance  $R = 0.012 \Omega$ , self-inductance  $L = 0.5 \mu\text{H}$ , whereas a lumped capacitance  $C = 50 \text{ nF}$  is connected to make the system resonate at the nominal frequency  $f_0 = 1 \text{ MHz}$ .

The specific values of the circuit elements considered in this paper are related to metasurfaces currently used as prototypes in laboratory tests. In general, the resonator resistance and self- and mutual inductances depend on the operating frequency due to skin and proximity effects, and these phenomena emphasize as the frequency increases. However, when considering resonators made of stranded-wire wound coils, those parameters can be considered frequency-independent up to a few MHz. In this condition, still considering the metasurface–unit cells perfectly resonant, it is possible to notice that the resistance and self- and mutual inductances depend on the system geometry only.

The distribution of the surface currents in 2D metasurfaces is dominated by the resonator mutual couplings and quality factor  $Q = \omega_0 L/R$ , whose impact is different depending on the lattice extension, as will be quantified later.

### 2.1 Effect of the resonator quality factor on the current distribution

At a fixed frequency, different quality factors lead to different current distributions and this effect can be particularly evident as the extension of the metasurface increases.

Considering a full impedance matrix  $\hat{\mathbf{Z}}_M$  (all coils interact), for low-quality factors (i.e.  $Q < 100$ ), obtained by increasing the resonator resistance, the resonators laying on the diagonal of the lattice experience higher currents [see [Figure 2\(a\)](#), showing the current magnitude of a  $51 \times 51$  surface characterized by  $Q = 40$ ] if compared with the off-diagonal ones.

In addition, the current gradually decreases from the resonators closer to the power source toward the boundary ones, which experience a nearly null current amplitude.

Reversely, as  $Q$  increases, it is difficult to predict and control the current distribution, as shown in [Figure 2](#), relative to the current magnitudes of a  $51 \times 51$  surface characterized by  $Q = 170$  and  $Q = 260$ , respectively. Indeed, while the central resonators still experience higher currents, the current distribution presents maxima and minima spread among all the lattice unit cells, whose locations are not known a priori. Intuitively, the abovementioned behavior can be explained considering that the current distribution originates from the fed resonator (the central one in this case) and spreads to surrounding unit cells, thanks to their mutual couplings, limited by the resonator resistance. A lower quality factor leads to stronger attenuation of the currents and, as a limit case, no current flows in the resonators furthest from the powered one: in this condition, they do not affect the current distribution. In case of higher quality factors, all the unit cells contribute to the resulting current distribution.

Accordingly, for a fixed  $Q$ , a wider metasurface (i.e. composed by more resonators) is characterized by resonators on the diagonal with higher current magnitude. This can be appreciated by comparing the plots of [Figure 2](#), in which the current distribution is shown for metasurfaces  $51 \times 51$  and  $101 \times 101$ , respectively, whose resonators have  $Q = 260$ .

It is therefore clear that the current distribution is influenced by both the number of resonators and their quality factor.

Based on the previous qualitative analysis, the ratio  $Q/N$  can be introduced: given a metasurface characterized by  $Q_1$  and  $N_1$ , to have a similar attenuation pattern with a surface of dimension  $N_2$ , a quality factor  $Q_2$  such that  $Q_1/N_1 = Q_2/N_2$  is needed. [Figure 3](#) shows the

---

## Analysis of current distribution

---

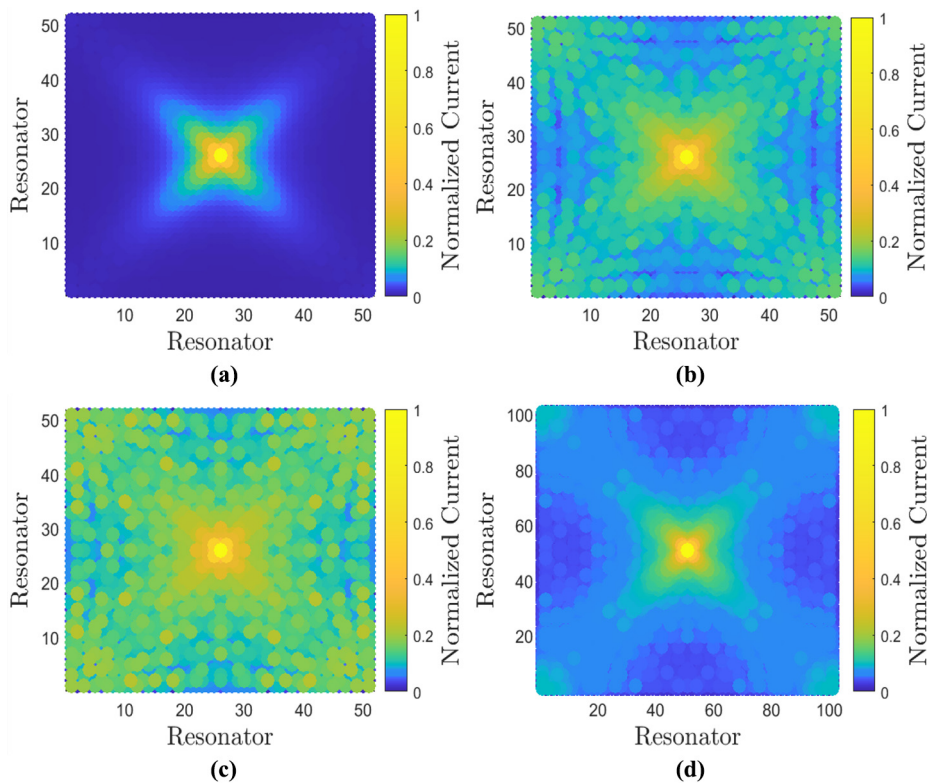
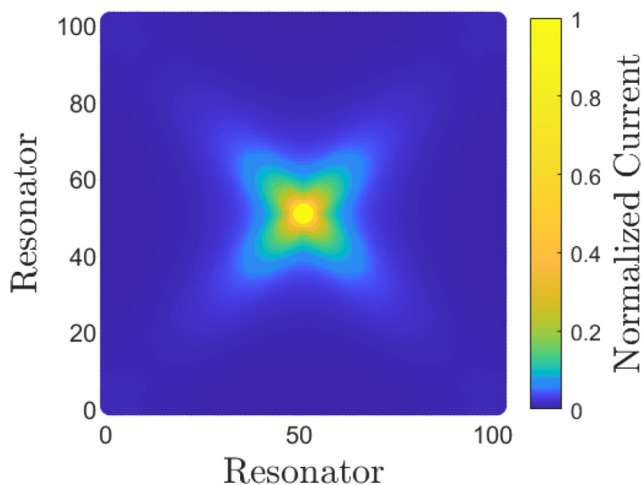


**Figure 2.** Current distribution of a metasurface excited in the central resonator at the frequency  $f_0$  considering the interaction between all coils in case of (a)  $51 \times 51$  metasurface with  $Q = 40$ ; (b)  $51 \times 51$  metasurface with  $Q = 170$ ; (c)  $51 \times 51$  metasurface with  $Q = 260$  and (d)  $101 \times 101$  metasurface with  $Q = 260$

---

Source: Figure created by authors



Source: Figure created by authors

**Figure 3.** Current distribution of a metasurface excited in the central resonator at the frequency  $f_0$  considering the interaction between all coils in case of  $101 \times 101$  metasurface with  $Q = 80$

---

current distribution of a metasurface with  $N = 101 \times 101$  resonators and  $Q = 80$  that can be compared with [Figure 2\(a\)](#), characterized by the same  $Q/N$  ratio; the similarity can be easily verified.

*2.2 Effect of couplings on current distribution*

Different models can be adopted to describe the metasurface behavior. Although the most accurate evaluation of the current distribution can be obtained considering the full impedance matrix, simplified models allow a dramatic reduction of the computational effort and also provide useful theoretical insight considering the analogy with waves. The models are compared considering  $51 \times 51$  metasurface (referred to as “high dimension”) with low  $Q$  resonators to emulate an infinitely extended lattice (as discussed in Subsection 2.1) and a  $5 \times 5$  metasurface (referred to as “low dimension”) with high  $Q$  resonators as a case study of practical interest.

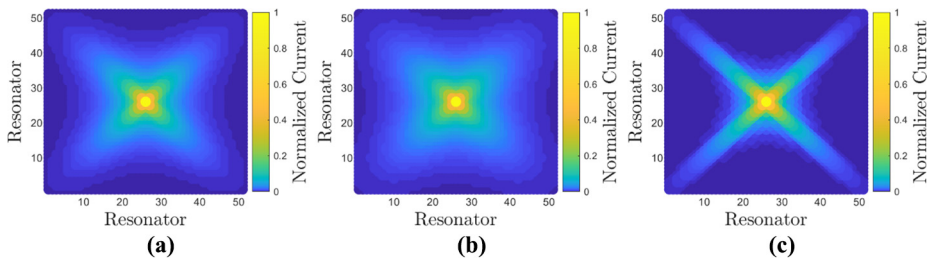
The evaluation a metasurface of small size ( $5 \times 5$ , in our case) is due to the fact that in practical applications ([Brizi et al., 2020](#); [Barmada et al., 2022](#); [Ojukwu et al., 2022](#), the extension of the metasurface is limited and the unit cells are designed to present high  $Q$  to avoid losses; it is consequently difficult to predict and control the current amplitude distribution.

*2.2.1 All couplings between coils (full model).* When all the couplings between coils are considered, the impedance matrix  $\mathbf{Z}_M$  is fully populated and the resulting current distribution is depicted in [Figures 4\(a\)](#) and [5\(a\)](#) with zoomed views in [Figures 6\(a\)](#) and [7\(a\)](#) for  $51 \times 51$  metasurfaces with  $Q = 25$  (low-quality factor) and  $Q = 170$  (high-quality factor), respectively; in [Figures 8\(a\)](#) and [9\(a\)](#), a low-dimension lattice is considered, with low and high  $Q$ , respectively. The currents are normalized with respect to the one of the central resonator, which presents the highest value. Besides the center, the local maximum values for the current are on the diagonal resonators in case of a high dimension metasurface, and the phenomenon is more evident for low  $Q$ .

In the  $5 \times 5$  metasurface (shown in [Figures 8](#) and [9](#)), the current maxima are also found in the resonators on the middle of the edges and this effect is more evident for high  $Q$  [see [Figure 9\(a\)](#)]. Moreover, in this case, minima of the amplitude of the current are found in some resonators on the diagonal. In the case of low  $Q$ , the maxima are always experienced by the resonators on the diagonal.

*2.2.2 Nearest-neighbor approximation and adjacent-diagonal couplings.* Considering that the mutual inductance between two coils dramatically decreases as their distance increases, the

**Figure 4.** Current distribution of a  $51 \times 51$  metasurface with  $Q = 25$ , excited in the central resonator considering (a) all couplings between coils; (b) the nearest neighbor approximation and adjacent-diagonal couplings and (c) the nearest neighbor approximation



**Note:** The values have been normalized to the current of the central resonator

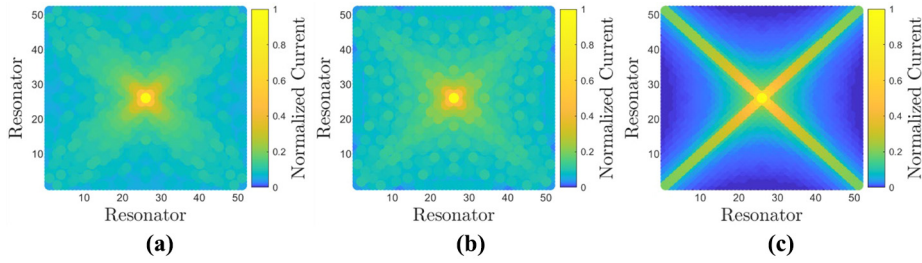
**Source:** Figure created by authors

mutual coupling coefficient between “distant” coils can be neglected. The quantification of “distant” leads to the definition of different degrees of approximation.

In the nearest neighbor approximation and adjacent-diagonal couplings approach, the couplings between nonadjacent resonators are neglected, i.e. only the couplings between adjacent resonators in all ( $x$ ,  $y$  and diagonal) directions is considered; practically speaking, each resonator is coupled only to the eight nearest resonators. The matrix  $\mathbf{Z}_M$  is, as a consequence, extremely simplified.

The current distribution is governed by the resonator mutual coupling  $M_{\text{adj}} = -50$  nH along the  $x$  and  $y$  directions and  $M_{\text{diag}} = -8.6$  nH along the diagonal directions.

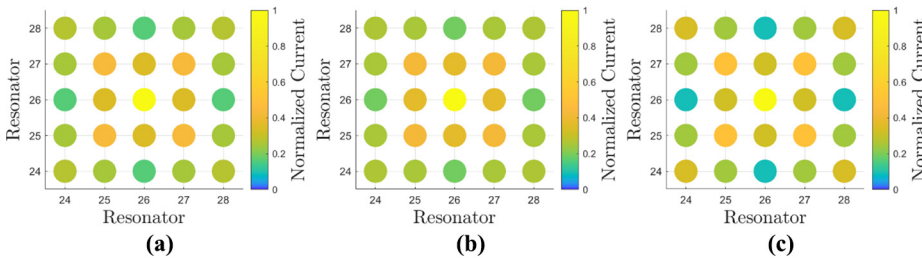
The current distribution obtained with this approximation is shown in Figures 4(b) and 5(b) with zoomed views in Figures 6(b) and 7(b) for the  $51 \times 51$  metasurfaces with  $Q = 25$  (low-quality factor) and  $Q = 170$  (high-quality factor), respectively. In Figures 8(b) and 9(b), the current distribution of the  $5 \times 5$  metasurface with  $Q = 25$  and  $Q = 170$  is shown, respectively.



**Note:** The values have been normalized to the current of the central resonator  
**Source:** Figure created by authors

## Analysis of current distribution

**Figure 5.** Current distribution of a  $51 \times 51$  metasurface with  $Q = 170$ , excited in the central resonator considering (a) all couplings between coils; (b) the nearest neighbor approximation and adjacent-diagonal couplings and (c) the nearest neighbor approximation



**Note:** The values have been normalized to the current of the central resonator  
**Source:** Figure created by authors

**Figure 6.** Current distribution in the central resonators (zoomed view) of a  $51 \times 51$  metasurface with  $Q = 25$ , excited at its center considering (a) all couplings between coils; (b) the nearest neighbor approximation and adjacent-diagonal couplings and (c) the nearest neighbor approximation

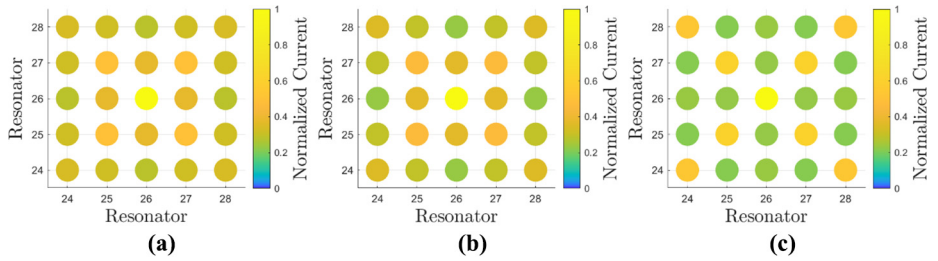
For the high and low  $Q$  metasurfaces [see Figure 4(b)], the current still distributes along the diagonals, although this behavior is less pronounced than in the previous case, whereas a higher  $Q$  leads to additional localized maxima and minima [see Figure 5(b)]. In the small lattice with high  $Q$ , the spread between the maxima and minima is emphasized, whereas it is limited in case of low  $Q$  [see Figures 8(b) and 9(b)].

2.2.3 *Nearest-neighbor approximation and magneto-inductive waves.* Being  $M_{\text{adj}} > M_{\text{diag}}$ , a further approximation consists in neglecting the coupling between coils along the diagonal. With this assumption, referred to as “nearest neighbor” approximation,  $\hat{\mathbf{Z}}_M$  further simplifies and the distribution of the currents is governed by the resonator-mutual couplings along the  $x$  and  $y$  directions of the space only, i.e. each resonator is coupled only to the nearest four resonators.

With this approximation the currents of resonators lying on the lattice diagonals markedly present the higher values for both the considered metasurfaces, as it is shown in Figures 4(c) and 5(c) with zoomed views in Figures 6(c) and 7(c) for metasurfaces with small

**Figure 7.**

Current distribution in the central resonators (zoomed view) of a  $51 \times 51$  metasurface with  $Q = 170$ , excited at its centre considering (a) all couplings between coils; (b) the couplings between adjacent coils in the  $x$ ,  $y$  and diagonal directions and (c) the nearest neighbor approximation

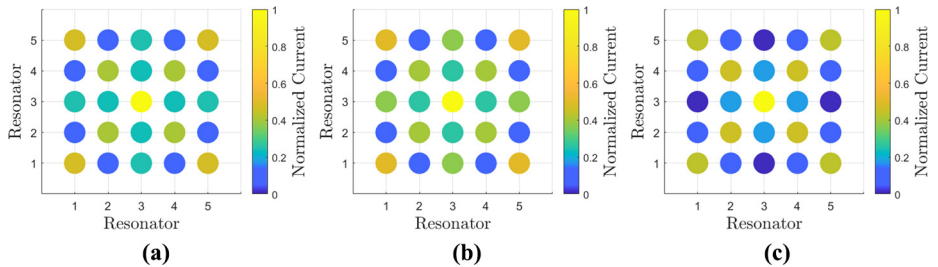


**Note:** The values have been normalized to the current of the central resonator

**Source:** Figure created by authors

**Figure 8.**

Current distribution of a  $5 \times 5$  metasurface excited in the central resonator with  $Q = 25$ , considering (a) all couplings between coils; (b) the nearest neighbor approximation and adjacent-diagonal couplings and (c) the nearest neighbor approximation



**Note:** The values have been normalized to the current of the central resonator

**Source:** Figure created by authors

( $Q = 25$ ) and large ( $Q = 25$ ) quality factors, respectively. In Figure 8(c), the currents of a small lattice with low  $Q$  are shown.

Under this approximation, the current distribution can be considered the result of the propagation of a current wave named “magneto-inductive” wave 0; the current wave attenuation is proportional to the resistance  $R$  of each unit cell and becomes stronger as the coupling between the resonators weakens.

The formulation is based on the analogy between the two-port networks of transmission lines and mutual coupled inductors, for which the input and output currents are delayed by  $\pi/2$  radians (due to the mutual impedance  $j\omega M$ ) and attenuated by the coil resistance. Intuitively, the current wave originates from the coil connected to the power source and, due to the mutual coupling, it propagates to the other resonators. To complete a  $2\pi$  rotation, four consecutive (coupled) resonators are needed. This clearly implies that the wavelength of MI waves is four times the length of a resonator edge  $\lambda_{MIW} = 4d$ . It is crucial to remind that this kind of waves are defined considering the coupling between adjacent cells only (Shamonina *et al.*, 2002).

A wave-based model allows a clear explanation of the obtained results when the metasurface emulates an infinite lattice, while it appears inaccurate in the case of small and weakly attenuated metasurface.

The current distribution can be considered the result of the superposition of forward and backward current waves, where the latter originate at the boundary of the metasurface.

As it happens in finite traditional waveguides, standing wave patterns can arise, leading to local maxima and minima of the current (Simonazzi *et al.*, 2022). To appreciate the propagation of the current wave, backward waves have to be avoided, which is possible if the waveguide is matched or infinitely long. However, to the best of the authors’ knowledge, it has not been clarified how to match a 2D lattice. Comparing Figures 6(c) and 7(c) with Figures 8(c) and 9(c), we can once again notice that the nearest neighbor approximation is effective for resonators with low  $Q$ , where the attenuation dominates.

### 3. Termination impedances for uniform current distribution

Being the choice for the termination conditions of a 2D structure not straightforward (Chan and Stevensy, 2011) and the nearest neighbor approximation as used in Solymar and Shamonina (2009) not always satisfying for metasurfaces with a limited number of elements, both a theoretical study and an optimization procedure are proposed.

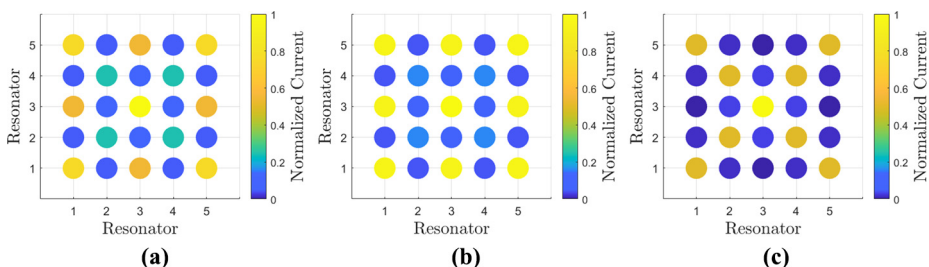


**Figure 9.** Current distribution of a  $5 \times 5$  metasurface excited in the central resonator with  $Q = 170$ , considering (a) all couplings between coils; (b) the nearest neighbor approximation and adjacent-diagonal couplings and (c) the nearest neighbor approximation

**Note:** The values have been normalized to the current of the central resonator

**Source:** Figure created by authors

3.1 Uniform current distribution in 2D lattices

Modeling the system based on the circuit theory clearly requires the KVLs are fulfilled. Hence, the basic requirements for the currents of magnetic metasurfaces are derived. At first, it must be noticed that the straightforward enforcement of KVL allows a uniform phasor current distribution only operating out of resonance, and may require different tuning and design for the meta-atoms.

Let  $\hat{I}$  be the phasor current value of the square lattice meta-atoms. The KVL for a generic meta-atom in the position  $mn$  can be written as:

$$0 = \hat{Z}_{mn}\hat{I}_{mn} + \sum_{\substack{i=1 \\ i \neq m}}^N \sum_{\substack{k=1 \\ k \neq n}}^N j\omega M_{mn,ik}\hat{I}_{jk} \quad (4)$$

where  $\hat{Z}_{mn}$  is the self-impedance of the coil at the position  $mn$  and  $M_{mn,ik}$  is the mutual induction coefficient between coils at the positions  $mn$  and  $ik$ .

Assuming the same phasor current  $\hat{I}$  for all the resonators, (4) becomes:

$$\hat{Z}_{mn} = -j\omega \sum_{\substack{i=1 \\ i \neq m}}^N \sum_{\substack{k=1 \\ k \neq n}}^N M_{mn,ik} \quad (5)$$

The right hand side (RHS) term of (5) is imaginary, whereas the left hand side (LHS) term of (5) is characterized by both a resistive and a reactive part. For this reason, the necessary condition to have uniform phasor current is  $\text{Re}[\hat{Z}_{mn} = 0]$ , i.e. a lossless system. This condition has a physical rationale, since only in a lossless system it is possible to have nonattenuated currents in all coils.

The same holds when all unit cells are tuned at the same resonant frequency  $f_0$  and (5) reduces to:

$$\text{Re}[\hat{Z}_{mn}] = -j\omega_0 \sum_{\substack{i=1 \\ i \neq m}}^N \sum_{\substack{k=1 \\ k \neq n}}^N M_{mn,ik} \quad (6)$$

which cannot be fulfilled being the LHS term real and the RHS term complex. Equations (5) and (6) clearly indicate that a lossy lattice with resonant unit cells does not allow a uniform current distribution.

*3.1.1 Lossless and low-loss metasurfaces.* Optimized metasurface coils are characterized by a high-quality factor, resulting in low-loss resonators. As first approximation, it is possible to neglect the resonator intrinsic resistance and consider a lossless behavior of the metasurface. Thus, from (5), the reactance of the generic cell  $X_{mn}$  that makes the current uniform is:

$$X_{mn} = -\omega \sum_{\substack{i=1 \\ i \neq m}}^N \sum_{\substack{k=1 \\ k \neq n}}^N M_{mn,ik} \quad (7)$$

Considering all cells tuned at the resonant condition, (7) yields  $X_{mn} = 0$ , consequently a uniform phasor current leads (again) to a violation of the KVL, as it is shown in (8).

It must be recalled at this point that (5) was obtained from (4) by imposing  $\widehat{I}_{mn} = \widehat{I}_{jk} = \widehat{I}, \forall m, n, j, k$ : as a consequence. This imposition leads to an impossible solution for lossy and lossless systems. Besides the trivial solution of (4) where  $\widehat{I} = 0$  in a 2D uniform square lattice, (8) is not verified, having all the mutual inductance coefficients  $M_{mn}$  the same sign.

It is then clear that resonant meta-atoms of a lossless square lattice can experience either the same current magnitudes or the same phases, but not both of them:

$$0 = -\omega_0 \sum_{\substack{i=1 \\ i \neq m}}^N \sum_{\substack{k=1 \\ k \neq n}}^N M_{mn,ik} \quad (8)$$

*3.1.2 Nearest neighbor approximation.* In the nearest neighbor approximation, it is assumed that resonators are coupled with their nearest ones only. In a square lattice, four couplings are then considered for a generic resonator out of the boundary and are characterized by the same mutual inductance  $M$ . In general, the condition (5) dramatically simplifies to:

$$\widehat{Z}_{mn} = -4j\omega M \quad (9)$$

which indicates that the overall impedance has to compensate for the induced voltage by near unit cells. It must be noticed, however, that this condition cannot be anyway satisfied in case of perfect resonance operation for either lossy or lossless systems.

### 3.2 Uniform current magnitude distribution in 2D lattices: the use of termination impedances

In the previous sections, we demonstrated that, under the hypothesis here adopted, a uniform distribution of the current (magnitude and phase) is not achievable, at least from a theoretical point of view. In practical applications, considering the tolerances of the lumped components and the realization of the resonators, distributions that can be considered “almost uniform” might be achieved, but are strongly case-dependent.

In this section, the authors investigate the possibility of obtaining a uniform current magnitude in the resonators, neglecting the phase difference.

The phasor current of a generic cell in the position  $(mn)$  can be written as:

$$\widehat{I}_{mn} = I e^{j\varphi_{mn}} \quad (10)$$

where the current magnitude  $I$  is the same for all the metasurface resonators and  $\varphi_{mn}$  is the phase difference between the phasor current of the  $mn$ th resonator and the fed one. Then, the constraint can be found directly from (4) enforcing (10).

When considering a real behavior of the metasurface, the resistance cannot be neglected and (4) becomes:

$$\widehat{Z}_{mn} = -\frac{j\omega}{e^{j\varphi_{mn}}} \sum_{\substack{i=1 \\ i \neq m}}^N \sum_{\substack{k=1 \\ k \neq n}}^N M_{mn,ik} e^{j\varphi_{ik}} \quad (11)$$

while in case of perfect resonance operation the generic constraint reduces to:

$$\operatorname{Re}[\widehat{Z}_{mn}] = -\frac{j\omega_0}{e^{j\varphi_{mn}}} \sum_{\substack{i=1 \\ i \neq m}}^N \sum_{\substack{k=1 \\ k \neq n}}^N M_{mn,ik} e^{j\varphi_{ik}} \quad (12)$$

3.2.1 *Lossless and low-loss metasurfaces.* In case of a lossless metasurface,  $\operatorname{Re}[Z_{mn} = 0]$  and (11) turns into:

$$X_{mn} = -\frac{j\omega}{e^{j\varphi_{mn}}} \sum_{\substack{i=1 \\ i \neq m}}^N \sum_{\substack{k=1 \\ k \neq n}}^N M_{mn,ik} e^{j\varphi_{ik}} \quad (13)$$

which leads, in case of perfect resonance operations of the cells, to:

$$0 = \sum_{\substack{i=1 \\ i \neq m}}^N \sum_{\substack{k=1 \\ k \neq n}}^N M_{mn,ik} e^{j\varphi_{ik}} \quad (14)$$

The constraint (13) can be achieved with the proper cell tuning and allows the current phase distribution to be set as desired. However, in case of resonance operations, further parameters are required to enforce (14), due to the difficulty in controlling the currents phases. To avoid increasing the cell impedances and losses, it is possible to insert additional lumped impedances in the boundary resonators, so that the lattice can be terminated. The termination impedances can be then determined applying KVL. In particular, two different values are considered for the terminations of the boundary resonators, i.e. one for the corners and one for the resonators internal to the edges (as in [Figure 1](#)).

In general, for a resonator on the upper edge at the position ( $Nn$ ) of an  $N \times N$  (terminated) metasurface, it is possible to write:

$$0 = (jX_{Nn} + \widehat{Z}_{Ts}) \widehat{I}_{Nn} + j\omega \sum_{\substack{i=1 \\ i \neq N}}^N \sum_{\substack{k=1 \\ k \neq n}}^N M_{mn,ik} \widehat{I}_{ik} \quad (15)$$

where  $\widehat{Z}_{Ts}$  is the termination impedance of the boundary resonator in the lattice edges. Thus, assuming a uniform current distribution and perfect resonance operation, the termination impedance value can be found as:

$$\widehat{Z}_{Ts} = -\frac{j\omega}{e^{j\varphi_{Nn}}} \sum_{\substack{i=1 \\ i \neq N}}^N \sum_{\substack{k=1 \\ k \neq n}}^N M_{mn,ik} e^{j\varphi_{ik}} \quad (16)$$

Considering a resonator in the corner ( $NN$ ), the KVL can be written as:

$$0 = (jX_{NN} + \widehat{Z}_{Tc}) \widehat{I}_{NN} + j\omega \sum_{\substack{i=1 \\ i \neq N}}^N \sum_{\substack{k=1 \\ k \neq N}}^N M_{mn,ik} \widehat{I}_{ik} \quad (17)$$

with  $\widehat{Z}_{T_c}$  the corner termination impedance defined, in case of perfect resonance operation and uniform current magnitude, as:

$$\widehat{Z}_{T_c} = -\frac{j\omega}{e^{j\varphi_{NN}}} \sum_{\substack{i=1 \\ i \neq N}}^N \sum_{\substack{k=1 \\ k \neq N}}^N M_{mn,ik} e^{j\varphi_{ik}} \quad (18)$$

Analysis of  
current  
distribution

**3.2.2 Nearest-neighbor approximation.** The nearest neighbor approximation can lead to very simple and effective results, still considering the same mutual coupling  $M$ . In particular, it is possible to obtain a uniform current magnitude while resonators operate in perfect resonance. The so-obtained uniform magnitude is, however, theoretical, and can be far from the real situation depending on the validity of the nearest neighbor approximation.

Indeed, for a resonator on the corner in the position  $(NN)$  the KVL includes only two mutual terms and the  $\widehat{Z}_{T_c}$  can be defined as:

$$\widehat{Z}_{T_c} = -j\omega M \frac{e^{j\varphi_{N-1,N}} + e^{j\varphi_{N,N-1}}}{e^{j\varphi_{NN}}} \quad (19)$$

The simple assumption that matches (19) is to consider  $e^{j\varphi_{N-1,N}} = e^{j\varphi_{N,N-1}} = e^{j\varphi_{NN}} = e^{j\varphi}$  thus:

$$\widehat{Z}_{T_c} = -2j\omega M \quad (20)$$

Then, for a resonator on the edge, the termination impedance can be found from the KVL written for a boundary resonator coupled with the  $NN$ th one, for which a condition on the current phase has been already set. Considering a resonator in the position  $(N-1)$ , the termination impedance  $\widehat{Z}_{T_s}$  can be found as:

$$\widehat{Z}_{T_s} = -j\omega M \frac{e^{j\varphi_{N,N}} + e^{j\varphi_{N,N-2}} + e^{j\varphi_{N-1,N-1}}}{e^{j\varphi_{N,N}}} \quad (21)$$

The conditions for the phases can be set considering the constraint (21) and the previous assumption. Under the nearest neighbor approximation, (21) written for the resonator  $(N-1, N-1)$  becomes:

$$0 = \widehat{Z}_{T_s} e^{j\varphi_{N-1,N-1}} + j\omega M (e^{j\varphi_{N-1,N}} + e^{j\varphi_{N,N-1}} + e^{j\varphi_{N-1,N-2}} + e^{j\varphi_{N-2,N-1}}) \quad (22)$$

It must be noticed that it would be applied to any cell but we need to consider a cell coupled with the one for which some hypothesis has been already formulated, namely,  $(NN)$ .

Being  $e^{j\varphi_{N,N}} = e^{j\varphi_{N-1,N}} = e^{j\varphi_{N,N-1}} = e^{j\varphi}$  to fulfill the constraint (19), which can be applied for example to the resonator  $(N-1, N-1)$ , it must be  $e^{j\varphi_{N-1,N-2}} = e^{j\varphi_{N-2,N-1}} = -e^{j\varphi}$ , leading to:

$$\widehat{Z}_{T_s} = -j\omega M \quad (23)$$

#### 4. Termination impedances for uniform current distribution: determination by an optimization procedure

The numerical calculation of the termination impedances for achieving a uniform current distribution can be addressed as an optimization problem. In particular, the problem consists in finding the values of  $\widehat{Z}_{T_s}$  and  $\widehat{Z}_{T_c}$  that minimize the normalized standard

---

**COMPEL**

deviation  $\sigma_I$  of the resonator current magnitudes. Formally, it is a single-objective optimization problem of two complex variables and it can be expressed as:

$$\min_{\widehat{Z}_{T_s}, \widehat{Z}_{T_c}} \sigma_I \quad (24)$$

Thus, the objective function of the problem is the normalized standard deviation  $\sigma_I$ , which is defined as:

$$\sigma_I = \frac{1}{\mu_I} \sqrt{\frac{1}{N} \sum_k \left( |\widehat{I}_k| - \mu_I \right)^2} \quad (25)$$

where

$$\mu_I = \frac{1}{N} \sum_k |\widehat{I}_k| \quad (26)$$

is the mean value of the resonator current magnitudes. When  $\sigma_I \approx 0$ , the correspondent  $\mu_I$  can be considered the value of each resonator current magnitude  $I_k$ .

The problem is solved implementing a particle swarm optimization (PSO) algorithm (Kennedy and Eberhart, 1995), which found the value of the four varying parameters, namely, the real and imaginary parts of the edge and corner termination impedances. The calculation is performed considering a sinusoidal input voltage of 1 V at the frequency  $f_0$ . After a first heuristic evaluation of possible limits for the parameter values, the variation range of each variable was set to  $[-10, 10]$  to leave the algorithm free to operate.

The details about the PSO optimizations are listed in Table 1.

In addition, adaptive inertia is used and the initial position of the particles corresponds to a uniform density in the search domain.

For all the considered metasurfaces, it is found that the convergence is reached faster if the full model is used, at the cost of a higher residual  $\sigma_I$ .

The results are summarized in Table 2, in which the optimum values of  $\widehat{Z}_{T_s}$  and  $\widehat{Z}_{T_c}$  with the correspondent normalized standard deviation  $\sigma_I$  are reported for metasurfaces with different number of cells considering the three different system models discussed in Section 2.2. In particular, the normalized current distribution of the  $5 \times 5$  terminated metasurface is shown in Figure 10, which shows a great uniformity in the resonator currents. Overall, the lower residual values (few percent) of  $\sigma_I$  are obtained with the nearest neighborhood approximation, but similar results can be achieved with the  $5 \times 5$  metasurface regardless of the adopted model. As the size of the lattice increases, the uniformity of the resonator currents is more difficult to be achieved, as the cases of  $9 \times 9$  and  $21 \times 21$  metasurfaces

---

Dimension	Full model	Adjacent coupling	Nearest neighborhood
Swarm size	1,000	1,000	1,000
Iterations	319	417	291
Objective evaluation	320368	420336	292148

---

**Table 1.**  
PSO parameters

**Source:** Table created by authors

---

Dimension	$\hat{\mathbf{Z}}_{Ts}(\Omega)$	$\hat{\mathbf{Z}}_{Tc}(\Omega)$	$\sigma_1$
<i>Full model</i>			
5 × 5	-0.32 - j 0.12	0.57 - j 0.14	0.0061
9 × 9	-0.12 + j 0.19	0.43 + j 0.05	0.1926
21 × 21	-0.28 + j 0.28	-0.37 + j 0.24	0.1304
<i>Adjacent coupling</i>			
5 × 5	-0.32 - j 0.14	0.58 - j 0.14	0.0043
9 × 9	-0.12 + j 0.15	0.41 + j 0.06	0.1614
21 × 21	-0.28 + j 0.30	-0.42 + j 0.25	0.1120
<i>Nearest Neighborhood approximation</i>			
5 × 5	-0.02 + j 0.31	-0.01 + j 0.62	0.0001
9 × 9	-0.03 + j 0.31	-0.06 + j 0.62	0.0012
21 × 21	-0.06 + j 0.33	-0.21 + j 0.49	0.0510

Analysis of current distribution

**Table 2.** Termination impedances and residual evaluation

Source: Table created by authors

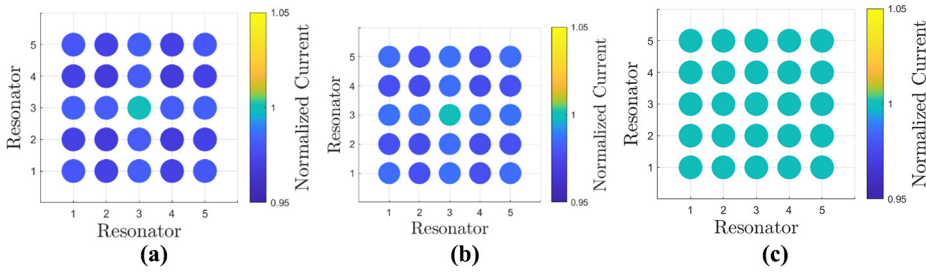


**Figure 10.** Current distribution of a 5 × 5 metasurface excited in the central resonator considering (a) all couplings between coils; (b) the couplings between adjacent coils in the x, y and diagonal directions and (c) the nearest neighborhood approximation

**Note:** The values have been normalized to the current of the central resonator  
**Source:** Figure created by authors

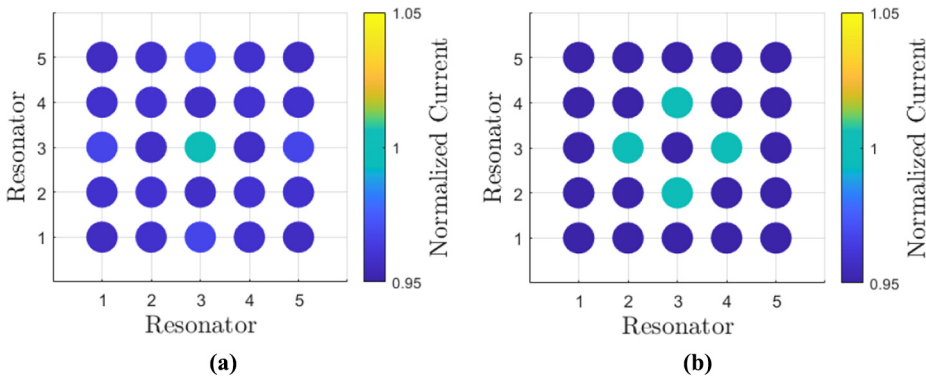


**Figure 11.** Current distribution of a 5 × 5 metasurface excited in the central resonator considering (a) all couplings between coils and termination impedance calculated by Adjacent coupling approximation; (b) all couplings between coils and termination impedance calculated by Nearest Neighbor approximation

Source: Figure created by authors

testify. It can be also noticed that similar values for the terminations are obtained when considering all the couplings or the adjacent couplings only, while they considerably deviate with the nearest neighborhood approximation.

The optimal impedance  $I$  (shown in Table 1) found by using Adjacent coupling and nearest neighborhood approximations have been tested also using the full model, and the results (for a  $5 \times 5$  metasurface) are shown in Figure 11. It is evident that metasurface simulated by the full model with  $\hat{Z}_{T_s}$  and  $\hat{Z}_{T_c}$  calculated by using the adjacent coupling model still gives a constant current (the termination impedances are very similar, as noted before), whereas the results with  $\hat{Z}_{T_s}$  and  $\hat{Z}_{T_c}$  calculated by using the nearest neighborhood coupling model leads to worse performances.

Moreover, the real part of the termination impedances, which is interpreted as a resistance, often results negative. In practical applications, this condition can be met by means of active devices only, such as OP-AMP-based circuits or thyristors. From our analysis, we noticed that within the realizations of the applied algorithm, suboptimal results can be obtained in terms of current's uniformity, resulting in termination impedances also having a positive real part, thereby indicating that passive components could be sufficient to terminate the lattice, at the cost of a lower current uniformity.

## 5. Conclusions

The nearest neighborhood approximation is usually adopted for the analysis of metamaterials, but the resulting current distribution is not accurate in case of arrays characterized by a relatively low number of unit cells. In this contribution, it is shown that at least the interaction between adjacent resonators should be considered to reduce the error. Both approximations introduce significant differences with respect to the full model that accurately represents mutual coupling between all coils. Nevertheless, the simplification obtained by neglecting the majority of the mutual coefficients leads to sparse matrices and it can be computationally convenient when high dimension systems are analyzed. However, their accuracy needs to be further investigated, especially in case of metasurfaces with a limited number of resonators.

A circuit-based analysis is carried out to obtain a uniform current's distribution on a finite size metasurface by the use of proper termination impedances, showing that a closed formula of limited practical usage can be obtained. Consequently, the uniform current's distribution obtained by applying a PSO algorithm has been shown for a test case  $5 \times 5$  array of resonators, proving that, with a certain degree of approximation, a very good uniformity can be obtained. Furthermore, the analysis has been applied to other two array sizes and the resulting termination impedances are found accordingly.

## References

- Baena, J.D., Bonache, J., Martin, F., Sillero, R.M., Falcone, F., Lopetegi, T., Laso, M.A., Garcia-Garcia, J., Gil, I., Portillo, M.F. and Sorolla, M. (2005), "Equivalent-circuit models for split-ring resonators and complementary split-ring resonators coupled to planar transmission lines", *IEEE Transactions on Microwave Theory and Techniques*, Vol. 53 No. 4, pp. 1451-1461.
- Barmada, S., Fontana, N., Sandrolini, L. and Simonazzi, M. (2022), "Optimal terminations of 2-D metasurfaces for uniform magnetic field applications", *IEEE Transactions on Magnetics*, Vol. 59 No. 5, pp. 1-4.
- Brizi, D., Fontana, N., Barmada, S. and Monorchio, A. (2020), "An accurate equivalent circuit model of metasurface-based wireless power transfer systems", *IEEE Open Journal of Antennas and Propagation*, Vol. 1, pp. 549-559.

- Chan, C.W. and Stevensy, C.J. (2011), "Two-dimensional magneto-inductive wave data structures", Proceedings of the 5th European Conference on Antennas and Propagation (EUCAP), *IEEE*, pp. 1071-1075.
- Glybovski, S.B., Tretyakov, S.A., Belov, P.A., Kivshar, Y.S. and Simovski, C.R. (2016), "Metasurfaces: from microwaves to visible", *Physics Reports*, Vol. 634, pp. 1-72.
- Kennedy, J. and Eberhart, R. (1995), "Particle swarm optimization", Proceedings of ICNN'95-international conference on neural networks, *IEEE*, Vol. 4, pp. 1942-1948.
- Lazzoni, V., Brizi, D. and Monorchio, A. (2023), "Spatial filtering magnetic metasurface for misalignment robustness enhancement in wireless power transfer applications", *Scientific Reports*, Vol. 13 No. 1, p. 560.
- Ojukwu, H., Seet, B.C. and Rehman, S.U. (2022), "Metasurface-aided wireless power transfer and energy harvesting for future wireless networks", *IEEE Access*, Vol. 10, pp. 52431-52450.
- Sandoval, F.S., Delgado, S.M.T., Moazenzadeh, A. and Wallrabe, U. (2019), "A 2-D magnetoinductive wave device for freer wireless power transfer", *IEEE Transactions on Power Electronics*, Vol. 34 No. 11, pp. 10433-10445.
- Simonazzi, M., Reggiani, U. and Sandrolini, L. (2022), "Standing wave pattern and distribution of currents in resonator arrays for wireless power transfer", *Energies*, Vol. 15 No. 2, p. 652.
- Shamonina, E., Kalinin, V.A., Ringhofer, K.H. and Solymar, L. (2002), "Magnetoinductive waves in one, two, and three dimensions", *Journal of Applied Physics*, Vol. 92 No. 10, pp. 6252-6261.
- Solymar, L. and Shamonina, E. (2009), *Waves in Metamaterials*, Oxford University Press, Oxford.

#### Corresponding author

Sami Barmada can be contacted at: [sami.barmada@unipi.it](mailto:sami.barmada@unipi.it)

---

For instructions on how to order reprints of this article, please visit our website:

[www.emeraldgrouppublishing.com/licensing/reprints.htm](http://www.emeraldgrouppublishing.com/licensing/reprints.htm)

Or contact us for further details: [permissions@emeraldinsight.com](mailto:permissions@emeraldinsight.com)